

# Mariner 10 stereo image coverage of Mercury

A. C. Cook

Center for Earth and Planetary Studies, National Air and Space Museum, Smithsonian Institution  
Washington, D. C.

M. S. Robinson

Department of Geological Sciences, Northwestern University, Evanston, Illinois

**Abstract.** A computer search was performed on all useable Mariner 10 images of Mercury for which refined camera positions and orientations are available. Over 2000 valid stereo pairs have been found. The results of this search allowed us to construct a map illustrating the available stereo coverage and the corresponding stereo height accuracy across the surface of Mercury. Examples are given to illustrate the quality of the available stereo pairs and the resulting digital elevation models.

## 1. Introduction

Mariner 10 made three flybys of Mercury between 1974 and 1975 and remains the only spacecraft to have visited this planet. During all three flybys the same hemisphere and illumination conditions were presented to the spacecraft. Many of the images overlap and were taken from widely separated viewpoints, thus providing stereo coverage. Example stereo images [Davies *et al.*, 1978] and a catalogue of stereo pairs [Jet Propulsion Laboratory (JPL), 1976] have been published. However, at the time that these stereo pairs were published, the camera position and orientation data were still preliminary, and we have found that some of these pairs have extremely weak stereo. Additionally, we find that many useful stereo pairs were never identified. Utilizing newly refined camera position and orientation data [Davies *et al.*, 1996; Robinson *et al.*, 1997, 1999a], we have compiled a new catalogue of stereo pairs and produced a map of stereo coverage.

Topographic information is an important resource for planetary scientists in the understanding of surface morphology and planetary geophysics. A digital elevation model (DEM) is needed when correcting images for illumination effects because it allows accurate calculation of incidence, emission, and phase angles on a pixel-by-pixel basis [Robinson *et al.*, 1999b]. Knowledge of topography also allows image rectification to be performed more precisely than by assuming a smooth ellipsoidal surface. Currently there are five sources of topographic information for Mercury:

1. Earth-based radar altimetry provides topographic profiles obtained within a band  $\pm 12^\circ$  of the equator [Harmon *et al.*, 1986]. Earth-based radar has the advantage of covering the equatorial zone in the hemisphere of Mercury that was not imaged by Mariner 10. However, these data have a coarse footprint size with a spatial uncertainty in the latitude direction of  $\sim 100$  km.

2. Limb profiles in Mariner 10 images reveal the presence of tall mountains; however, the height accuracy is dependent upon the pixel size of approximately  $\pm 1$  km.

3. Applying photogrammetry to Mariner 10 images [Hapke *et al.*, 1975; Mouginis-Mark and Wilson, 1981; Schenk and

Melosh, 1994; Watters *et al.*, 1998] provides the best resolution topographic measurements of Mercury. However, this method is most practical over small areas [cf. Davis and Soderblom, 1984; McEwen, 1991]. The technique has been demonstrated for producing DEMs of other solar system bodies [Kirk, 1987; Murray *et al.*, 1992; Giese *et al.*, 1996].

4. Shadow measurements [Malin and Dzurisin, 1977; Pike, 1988] allow for very accurate point measurements of relief but are restricted to within  $\sim 30^\circ$  of the terminator, at best, and yield only relative heights between the projecting landform and shadow edge. Images of the same area, taken from a fixed viewpoint, under many different illumination conditions, would be required in order to produce topographic maps using this technique.

5. Stereo images taken by Mariner 10 [Dzurisin, 1978; Malin, 1978; Thompson *et al.*, 1986; Watters *et al.*, 1998] cover large contiguous areas at moderate resolution. Using these images, the stereo technique provides the next best spatial resolution to photogrammetry, and topographic measurements can be related easily to features seen in images, unlike radar profiles.

## 2. Mariner 10 Mission and Data

The Mariner 10 mission [Murray and Burgess, 1977; Dunne and Burgess, 1978] was conceived in 1968 by the Science board of the National Academy of Science and approved by NASA in 1973. The spacecraft was built by the Boeing company, and the project was managed and run from the Jet Propulsion Laboratory (JPL). Mariner 10 was the first spacecraft to utilize a gravitational assist, at Venus, to both redirect the spacecraft and to change its velocity. The resulting saving in fuel mass allowed the spacecraft to carry a more extensive set of experiments to Mercury and to carry additional fuel sufficient enough for three flybys. Mariner 10's instruments included a triaxial fluxgate magnetometer, a scanning electrostatic analyzer and electron spectrometer, radio science and trajectory experiments, a two-channel infrared radiometer, an energetic particles experiment, an extreme ultraviolet spectrometer, and a pair of vidicon cameras [Danielson *et al.*, 1975; Murray, 1975; Murray and Burgess, 1977].

The spacecraft was launched from Cape Kennedy at 1445 UTC on November 2, 1973. It acquired images of the Earth just 16 hours after liftoff and imaged the Moon's northern

Copyright 2000 by the American Geophysical Union.

Paper number 1999JE001135.  
0148-0227/00/1999JE001135\$09.00

hemisphere less than one week later [Murray, 1975; Murray and Burgess, 1977; Dunne and Burgess, 1978]. Until the Galileo flyby of the Moon in 1992 [Belton *et al.*, 1994] these data represented the only multispectral data for the eastern limb and portions of the farside [Robinson *et al.*, 1992]. The swing-by of Venus took place on February 5, 1974, and it provided an excellent opportunity to image the planet both in UV wavelengths and at a higher spatial resolution than could be achieved from Earth.

During the first encounter with Mercury on March 29, 1974, at 2047 UTC, Mariner 10 passed within 705 km of the night-side, and more than 2300 images were obtained of the incoming and outgoing hemispheres [Murray, 1975] before and after closest approach. During the second encounter at 2159 UTC on September 21, 1974, the spacecraft passed within 48,069 km of the dayside, and another 750 images were captured, primarily of the southern hemisphere, in order to tie together the two separated regions imaged during the first encounter [Strom *et al.*, 1975; Murray and Burgess, 1977]. During the third, and final, encounter on March 16, 1975 (2239 UTC), Mariner 10 passed within 327 km of the nightside, and despite the fact that the tape recorder no longer worked and the high-gain antenna was inoperable, ~450 quarter-width 6-bit images were transmitted in real time. The close approach images were the highest resolution returned by Mariner 10, with ground pixel sizes as small as 100 m/pixel [Murray and Burgess, 1977; Dunne and Burgess, 1978]. Communication with the spacecraft was terminated on March 24, 1975, after its nitrogen supply was depleted and its radio transmitter was instructed to switch off. Mariner 10 remains in a solar orbit.

### 3. Available Images

Approximately 3500 images were taken during the Mercury encounters; however, the number of these images that we utilized is ~1000. Many of the original images are not useful because (1) some were unrecoverable from archive tapes, (2) others contained too many blank lines from corrupt tape blocks or original telemetry losses, (3) many images were too low in resolution, (4) some were taken of deep space, and (5) spacecraft position information is not available. The majority of the remaining images must undergo filtering with an iterative salt and pepper noise removal program [Soha *et al.*, 1975; Eliason and McEwen, 1990], resulting in a degradation of effective spatial resolution [Robinson *et al.*, 1999a]. Mariner 10 images were geometrically distorted by local magnetic fields and by electrostatic buildup in bright areas of the image which caused beam bending [Benesh and Morrill, 1973]. Hence for photogrammetric purposes the locations of calibration reseaux present in the vidicon images must be found, and a geometric correction must be performed. For cartographic purposes, images taken in any filter can be intermixed in a stereo pair because, like the Moon, Mercury does not exhibit large color contrasts. From refined camera position and orientation data [Robinson *et al.*, 1999a] we computed relative positions and orientations between the spacecraft and the surface for both images in each stereo pair. Additionally, we used the revised focal length values of 1494.3 mm and 1500.6 mm for cameras A and B, respectively [Robinson *et al.*, 1999a].

### 4. Definition of Good Stereo Pairs

Accurate topographic data may be extracted from pairs of images if the geometric parameters of acquisition are favor-

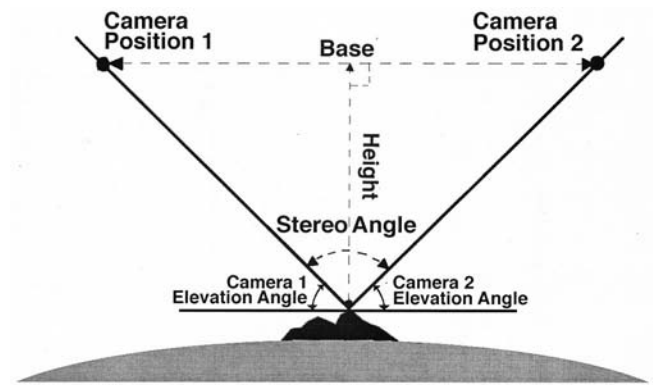


**Figure 1.** Simplified definition of stereo angle, base, and height. The stereo height accuracy  $A$  is defined as  $A = R_p K / (B/H)$ , where  $R_p$  is the poorest image resolution,  $K = 0.2$  (precision of measurement in pixels) for CCD cameras or  $K = 1.0$  for vidicon cameras such as the Mariner 10 cameras,  $B$  is the base, and  $H$  is the height.

able. For a fixed spacecraft height, as the distance (baseline) between the two camera positions becomes larger, the stereo angle (Figure 1) increases, and the resultant stereo measurements have a greater vertical accuracy. In each stereo pair, for a given longitude/latitude ( $\lambda$ ,  $\phi$ ) point on the planet's surface, a corresponding image displacement direction caused by a planetary surface vertical offset was determined. The measurement error in vidicon images can be regarded as  $\pm 0.5$  pixels [Cook *et al.*, 1992], therefore, using predicted positions for a surface point in stereo pair images and adding  $\pm 0.5$  pixel errors of measurement, the corresponding expected relative height accuracy for the surface can be computed.

A set of rules [Cook *et al.*, 1992, 1996] were devised based upon analysis of Viking Orbiter stereo images [Wu, 1978] of Mars and Clementine stereo images [Cook *et al.*, 1994a; Oberst *et al.*, 1996; McEwen and Robinson, 1997] of the Moon. The registration accuracy  $K$  for an image pair is a function of incidence angle, emission angle, signal-to-noise ratio (SNR), camera distortions, and variations in surface brightness (see Figure 1 for a definition of stereo terms). Experience has shown that for the Moon, with a CCD instrument and adequate SNR, images can be correlated to  $\sim K = 0.2$  pixels [Cook *et al.*, 1996, 2000]. However, for vidicons like those flown on Mariner 10 or the Viking Orbiters,  $K = 1$  [Cook *et al.*, 1992, 1997].

Using selection criteria derived from Viking images of Mars, we searched our Mariner 10 database to find matching pairs and to test the validity of the Mars parameters for Mercury. We used subroutines from a geographically indexed prototype database, the Solar System Information System, or SOLIS [Cook *et al.*, 1994b]. The source data were a file of updated camera positions and orientation data for the Mariner images [Davies *et al.*, 1996; Robinson *et al.*, 1999a]. This preliminary run yielded in excess of 3000 stereo pairs. Several examples of predicted stereo pairs could not be stereo matched though, despite the illumination conditions being similar. Examples of both valid and invalid pairs found during the initial run are presented below. From this preliminary run we defined new criteria for the Mariner 10 data set.

Figure 2 shows a stereo pair covering the region of Mercury around Bello crater in the H-7 Beethoven map sheet [Davies *et al.*, 1978]; one of the images was taken with a spacecraft ele-

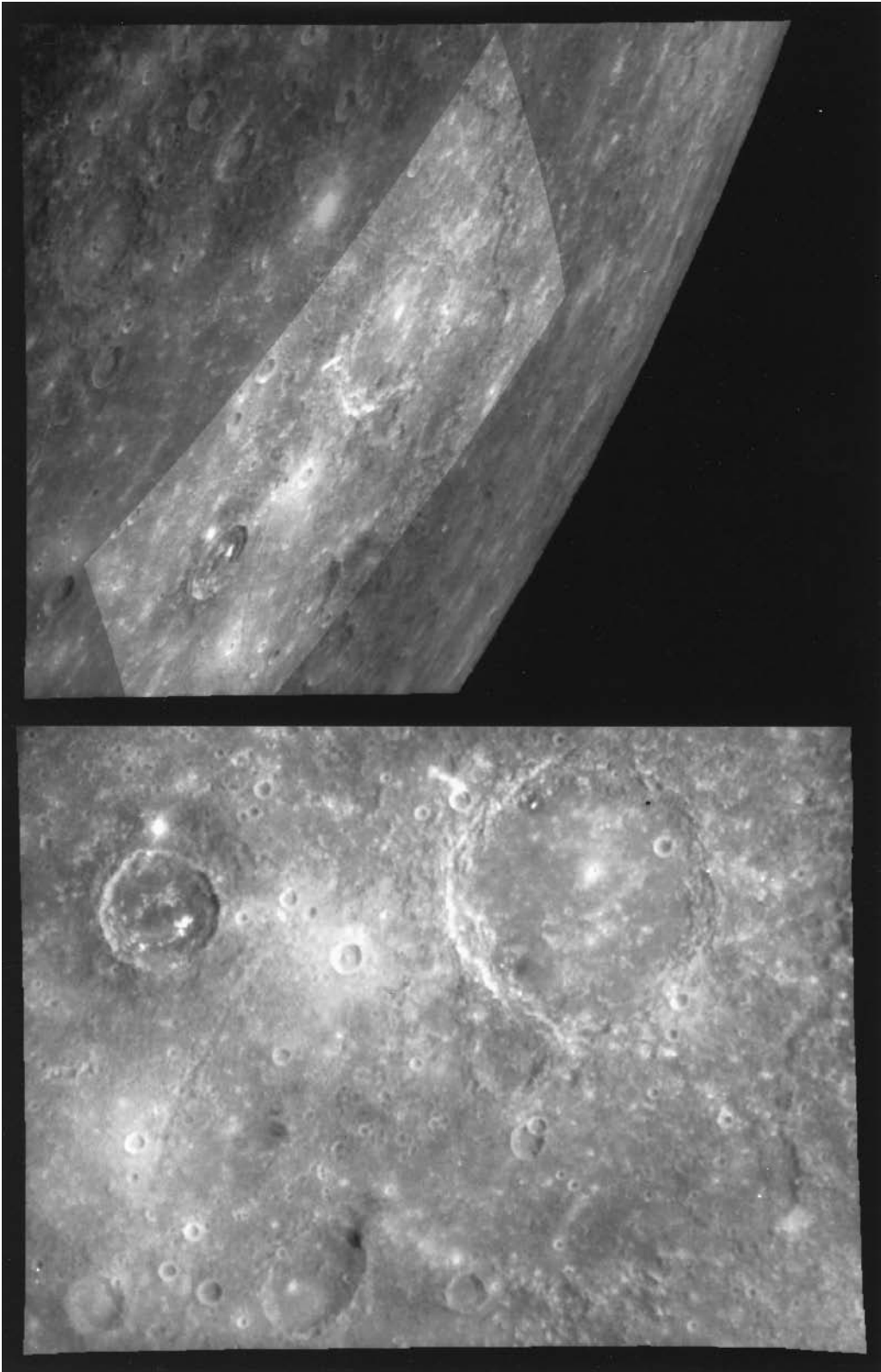


**Figure 2.** Common region of stereo coverage (indicated with lighter shading) between Mariner 10 Mercury images (top) 000207 and (bottom) 166815. The map sheet area is Beethoven H-7 (SW quadrant). At  $123^{\circ}\text{W}$ ,  $21^{\circ}\text{S}$ , the stereo angle is  $\sim 61^{\circ}$ , and the mean spacecraft elevation angle is  $\sim 51^{\circ}$ . The largest crater visible is named Bello (diameter 150 km).

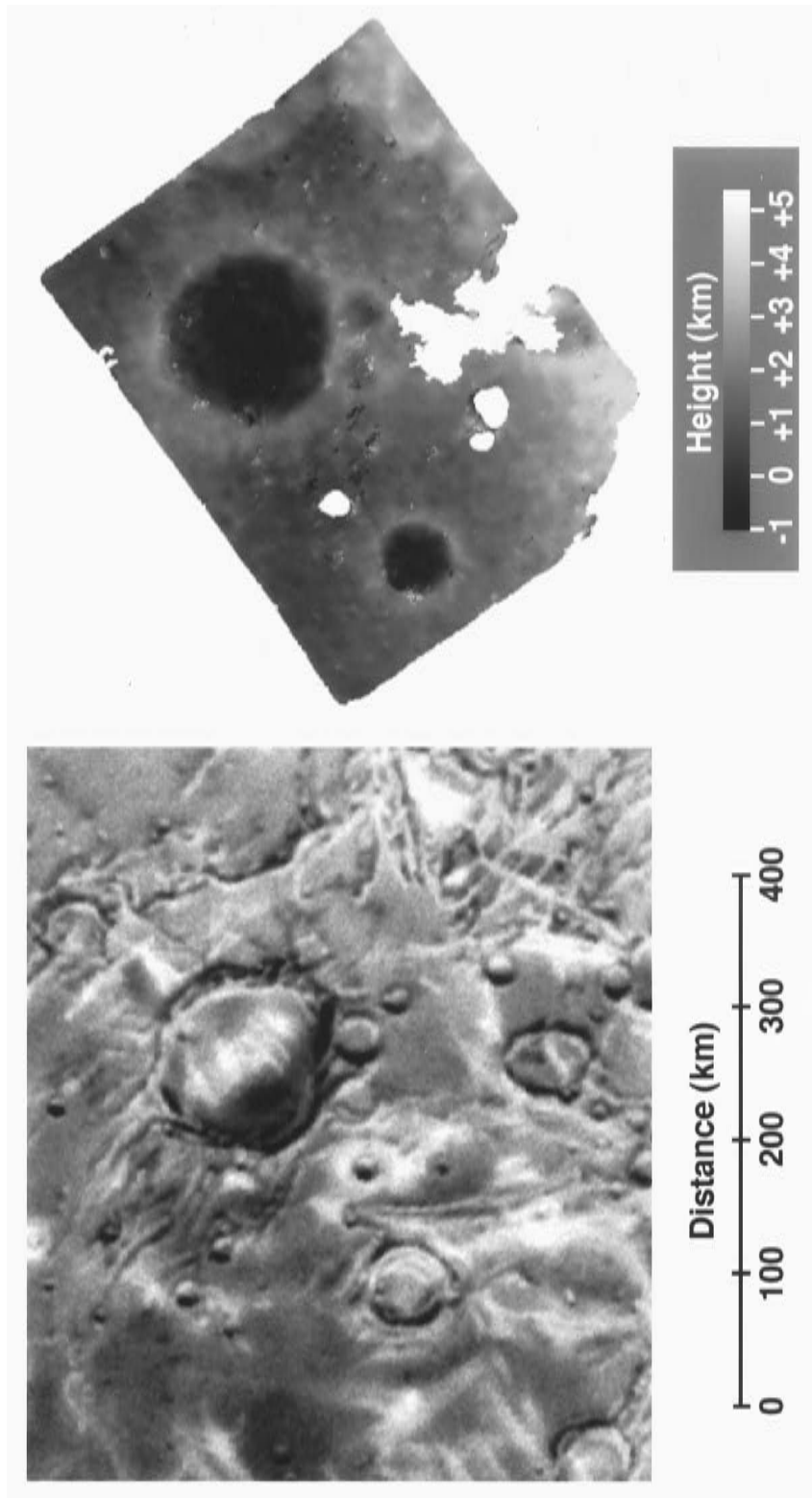


**Figure 3.** The general area ( $128^{\circ}\text{W}$ – $114^{\circ}\text{W}$ ,  $26^{\circ}\text{S}$ – $15^{\circ}\text{S}$ ) studied in Figure 2 can be seen in the airbrush map on the left. A gray scale DEM of the stereo-matched region can be seen on the right (white indicates areas that lie outside the stereo pair overlap or that could not be stereo matched reliably). Part of the Beethoven basin ring is located on the right of the DEM. The stereo height accuracy for a single matched point is  $\pm 460$  m.

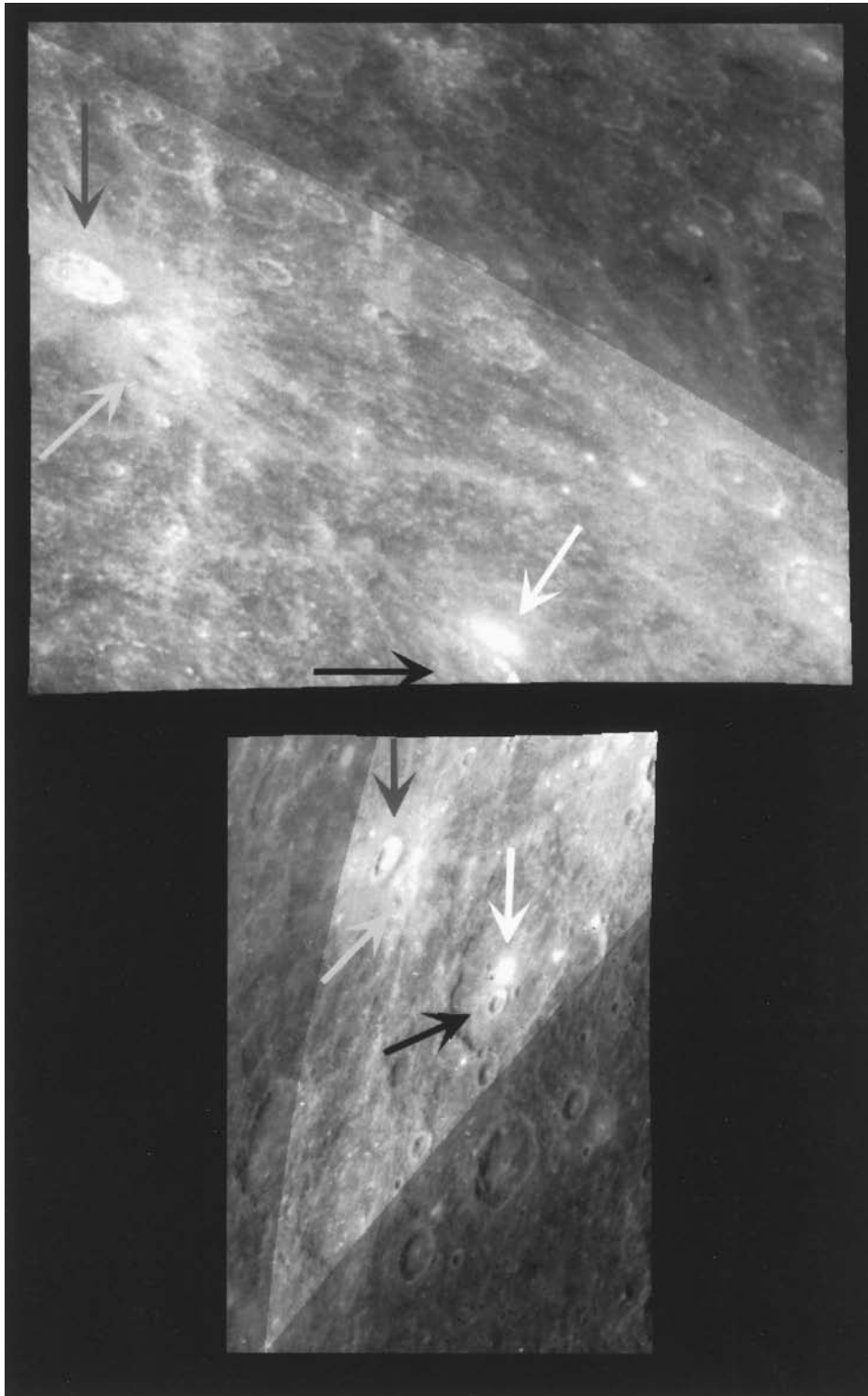


**Figure 4.** Common region of stereo coverage between Mariner 10 Mercury images (top) 166769 and (bottom) 166578. The map sheet area is Kuiper H-6 (NW quadrant). At  $69^{\circ}\text{W}$ ,  $0^{\circ}\text{N}$ , the stereo angle is  $69^{\circ}$ , the minimum spacecraft elevation angle is  $23^{\circ}$ , and stereo height accuracy is  $\pm 450$  m. The arrows indicate four examples of common features that can be recognized between these images: Most other common features are extremely difficult to identify in this viewing geometry.

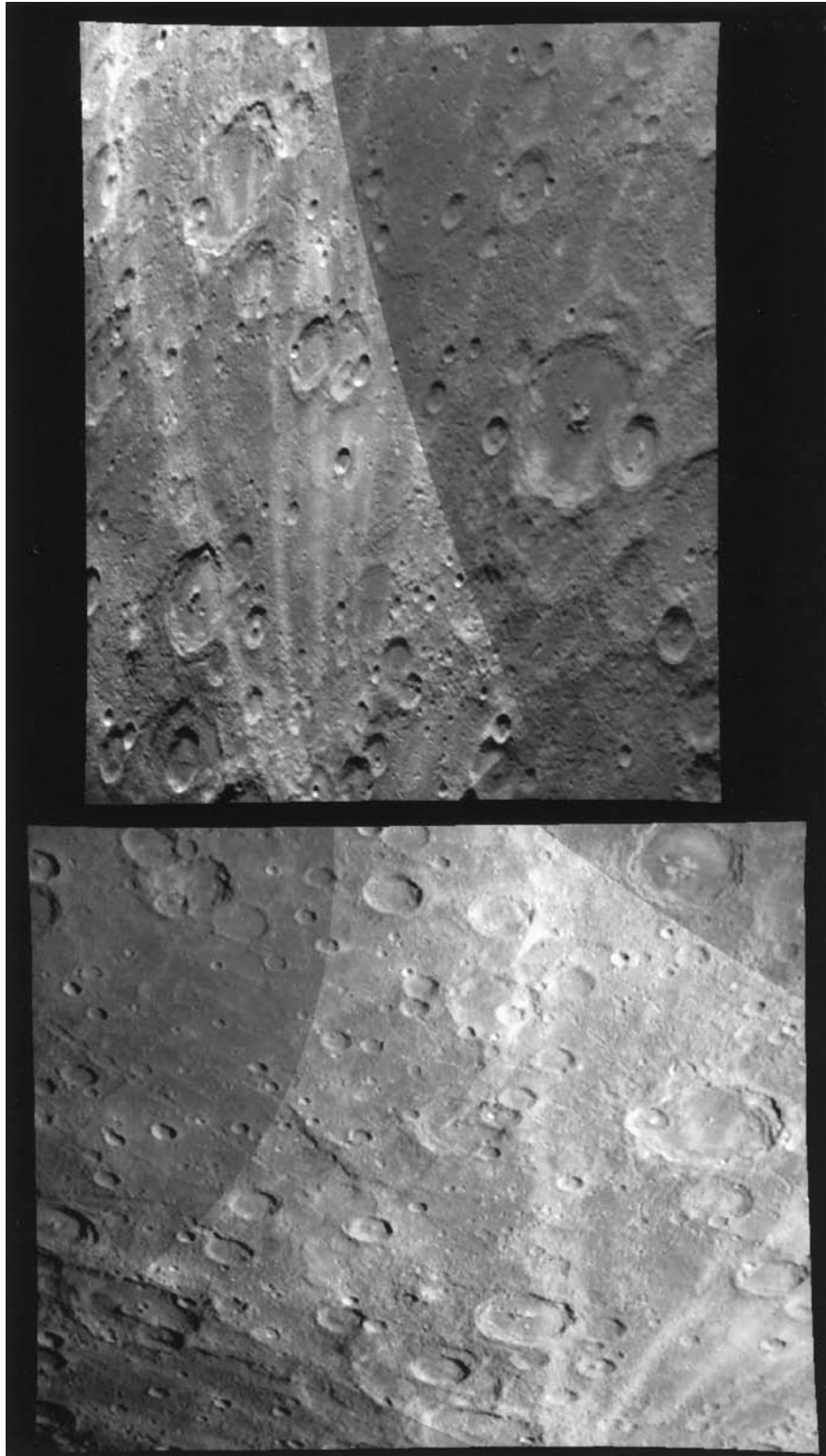


**Figure 5.** Example of an extreme stereo angle stereo pair that we were unable to match. It covers part of the Michelangelo map sheet H-12 and shows the common region of stereo coverage between Mariner 10 Mercury images (top) 166612 and (bottom) 027229. At  $142^{\circ}\text{W}$ ,  $63^{\circ}\text{S}$ , the stereo angle is  $\sim 107^{\circ}$ , and the mean spacecraft elevation angle is  $\sim 31^{\circ}$ . It is easier to identify common features between these two images. However, the differences in feature appearance are so large, because of topographic shielding, that these two images are extremely difficult to stereo match.

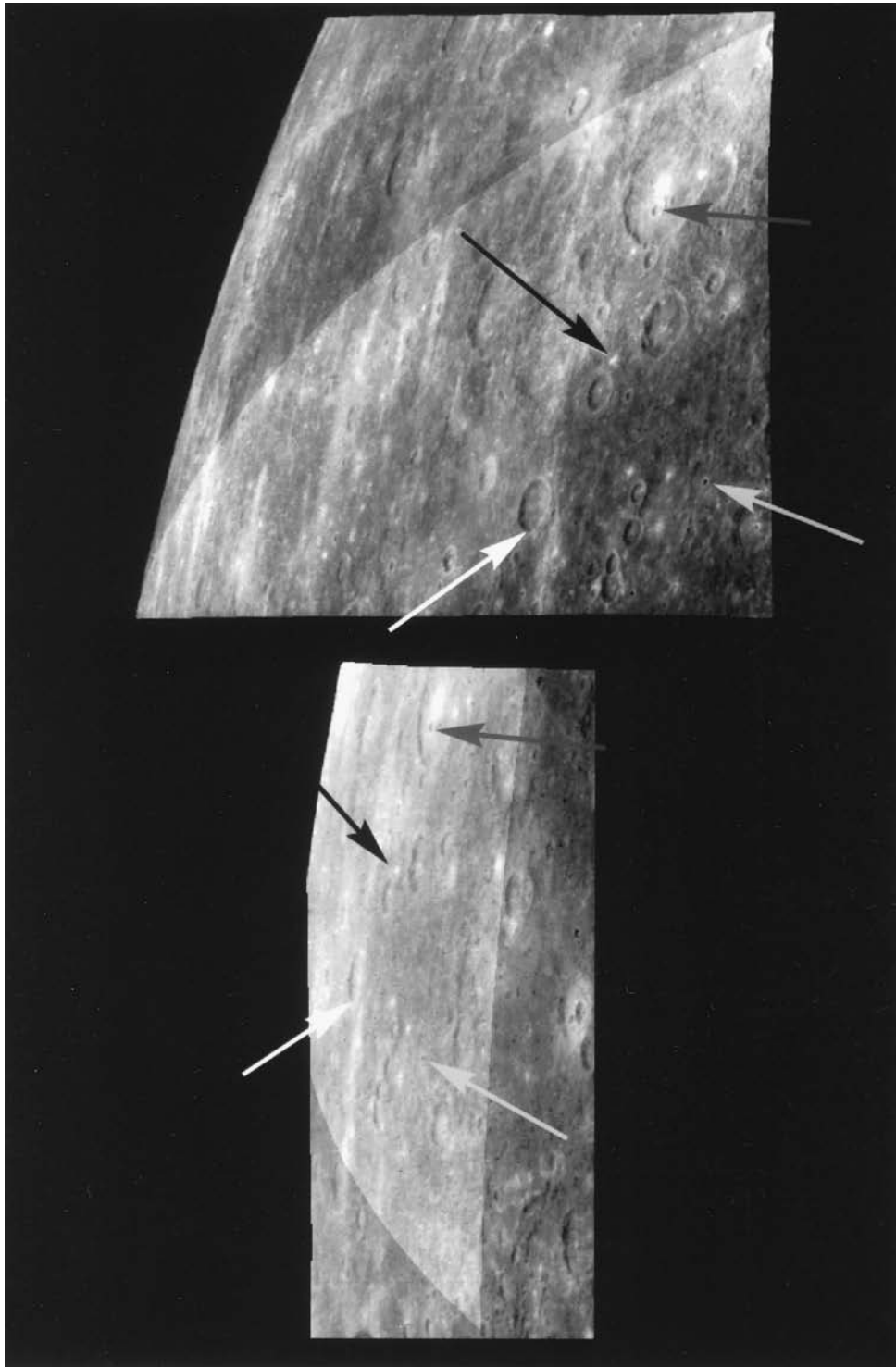


**Figure 6.** Common region of stereo coverage between Mariner 10 Mercury images (top) 166578 and (bottom) 027229. The map sheet area is Kuiper H-6 (NW quadrant). At  $69^{\circ}\text{W}$ ,  $0^{\circ}\text{N}$ , the stereo angle is  $\sim 12^{\circ}$ , and the mean spacecraft elevation angle is  $\sim 27^{\circ}$ . In this stereo pair several common features can be recognized (see arrows), and the pair can be stereo matched; however, the expected stereo height accuracy ( $\pm 830$  m) is quite poor.

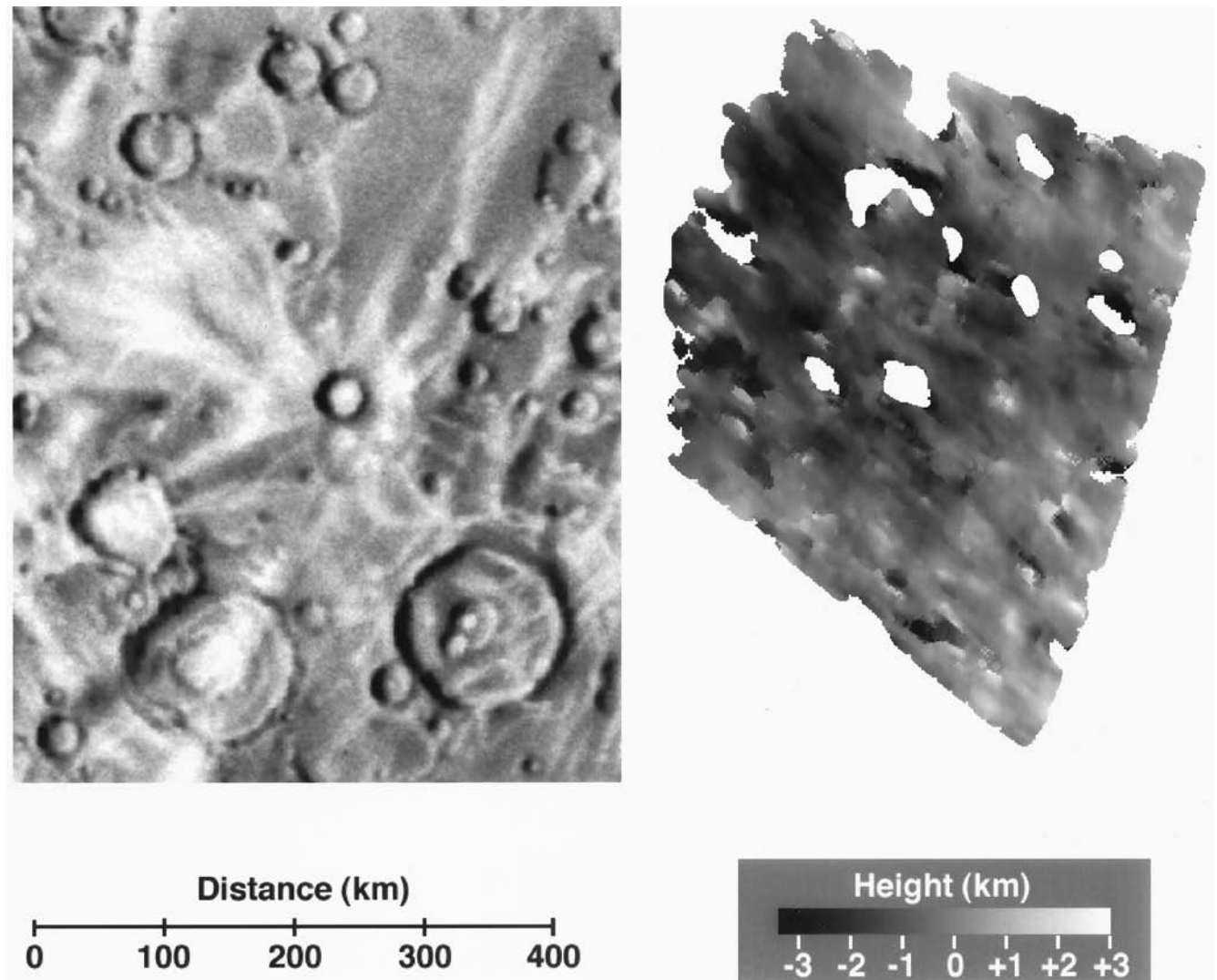


**Figure 7.** DEM produced from the poor height accuracy ( $\pm 830$  m) stereo pair shown in Figure 6. On the left is an airbrush map of the DEM region ( $77^{\circ}\text{W}$ – $66^{\circ}\text{W}$ ,  $11^{\circ}\text{N}$ – $3^{\circ}\text{S}$ ). On the right is a gray scale DEM of the stereo matched region (white indicates areas that lie outside the stereo pair overlap or that could not be stereo matched reliably). Although a nearly contiguous DEM has been produced, so much topographic noise is present that it is difficult to recognize surface features.

vation angle of  $\sim 22^{\circ}$  above the horizon (elevation angle is equivalent to  $90^{\circ}$  minus the emission angle). The stereo height accuracy for a typical single matched point was approximately  $\pm 460$  m. The derived DEM (Figure 3) has reasonably low topographic noise despite the low elevation angle in one of the images. However, a few regions could not be matched due to topographic shielding starting to interfere with the recognition of surface features under these low-elevation conditions. We therefore set a minimum spacecraft elevation angle limit of  $15^{\circ}$ . However, image pairs with elevation angles lying above this limit may sometimes prove unsuitable too. The stereo pair in Figure 4 has a minimum spacecraft elevation angle of  $\sim 23^{\circ}$  and a minimum stereo height accuracy of approximately  $\pm 450$  m (comparable to that shown in Figure 2); however, it did not yield a usable DEM. This is due to the large stereo angle of  $\sim 69^{\circ}$  combined with a low elevation angle. The resultant distortion from frame to frame and topographic shielding make it impossible for the stereo matcher to find reliable points. Likewise, for an image pair with a moderate elevation angle but

with an even larger stereo angle, the stereo matcher again fails for similar reasons (Figure 5: average elevation angle  $\sim 31^{\circ}$ , stereo angle  $\sim 107^{\circ}$ ). We have developed an approximate rule of thumb to aid in the selection of stereo pairs based upon the stereo and elevation angles: The stereo angle should be  $< 1.5$  times the mean elevation angle of the spacecraft in both images. Figure 6 shows an example of a stereo pair with a small stereo angle ( $12^{\circ}$ ) and a stereo height accuracy of approximately  $\pm 830$  m. Thus the DEM that results from matching this stereo pair (Figure 7) is of poor quality. However, in regions where no other stereo coverage exists, any available stereo pair where the height accuracy is better than  $\pm 1000$  m may be utilized to examine low-frequency topography. Figure 8 presents a stereo pair with overall favorable viewing parameters; the stereo angle is  $\sim 38^{\circ}$ , and the spacecraft was  $\sim 40^{\circ}$  in elevation in one image and  $\sim 55^{\circ}$  in the other. The stereo height accuracy for a single matched point is approximately  $\pm 370$  m. There are, however, still some minor topographic shielding effects at the foot of crater rims (Figure 9).

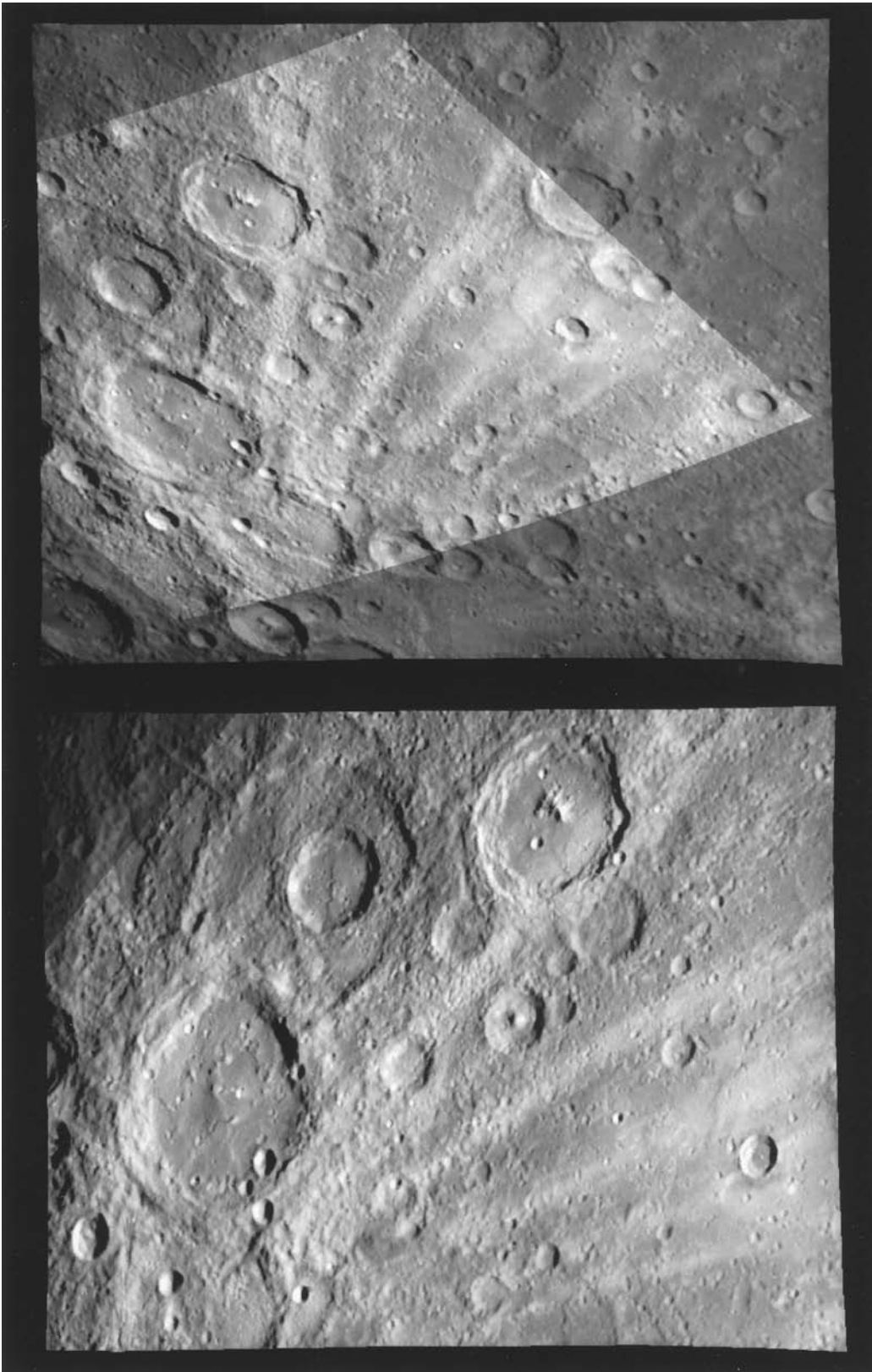


**Figure 8.** Common region of stereo coverage between Mariner 10 Mercury images (top) 166835 and (bottom) 166749. The area lies in the overlap between Michelangelo H-12 (SW quadrant) and Bach H-15 map sheets. At  $147^{\circ}\text{W}$ ,  $66^{\circ}\text{S}$ , the stereo angle is  $\sim 38^{\circ}$ , and the mean spacecraft elevation angle is  $\sim 48^{\circ}$ .

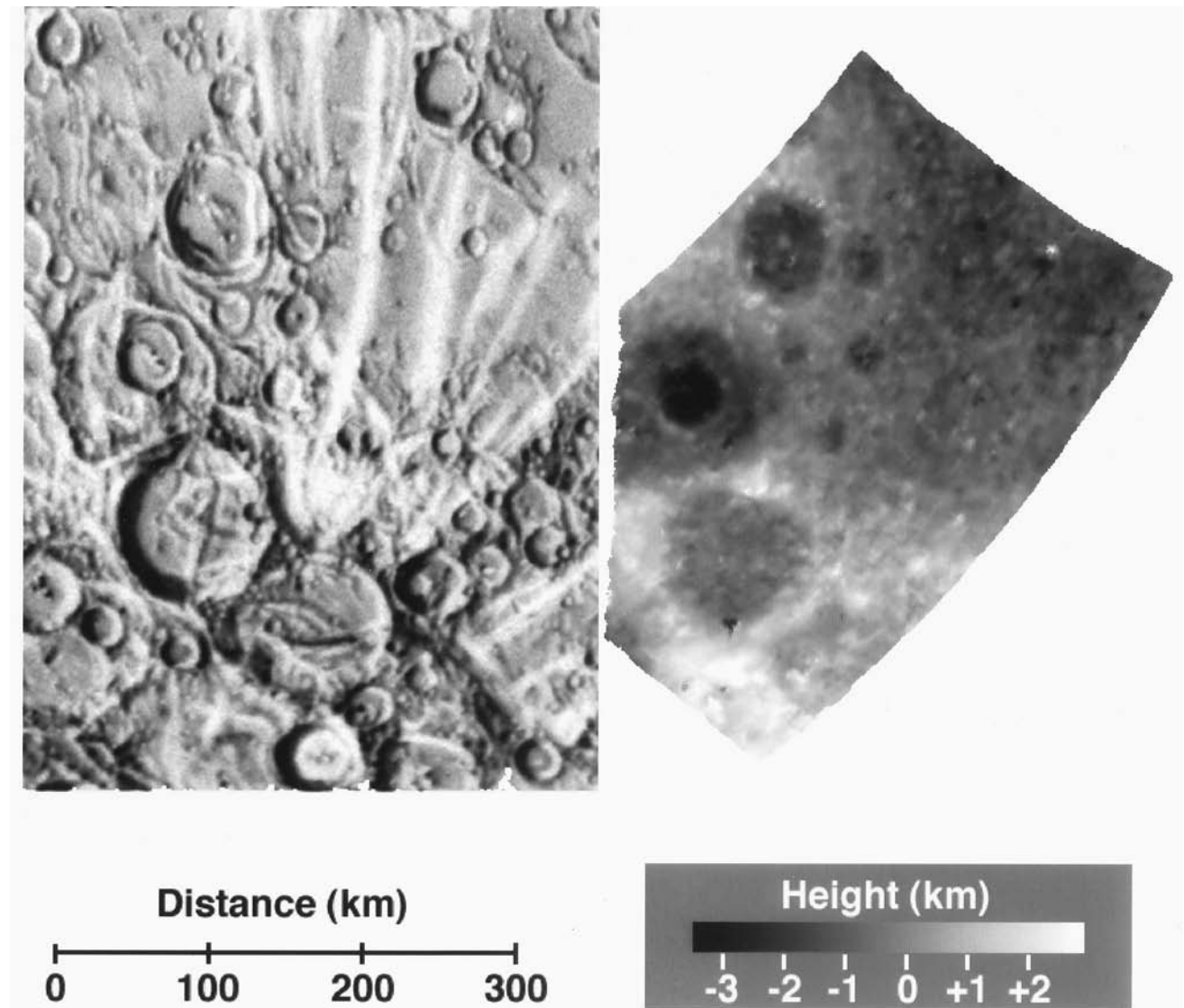


**Figure 9.** An airbrush map and DEM of the region of stereo overlap in Figure 8. On the left is an airbrush map of the stereo overlap region ( $156^{\circ}\text{W}$ – $133^{\circ}\text{W}$ ,  $72^{\circ}\text{S}$ – $60^{\circ}\text{S}$ ). On the right is the resulting gray scale DEM (white indicates areas that lie outside the stereo pair overlap or that could not be stereo matched reliably). At least seven craters are clearly visible. The stereo height accuracy for this pair is  $\pm 370$  m.

One of the best quality DEMs (Figure 10) that we have produced so far is of the Discovery Rupes area. The spacecraft has a minimum elevation angle of  $\sim 27^{\circ}$ , the stereo angle is  $\sim 41^{\circ}$ , and the stereo height accuracy for a single matched point is approximately  $\pm 570$  m. The resultant DEM has an excellent SNR and has proved useful for examining the Discovery Rupes lobate scarp feature [Watters *et al.*, 1998].

## 5. Final Stereo Search Parameters

After examining a subset of stereo pairs from the initial stereo search parameters (see examples given in section 4), parameters relevant to the Mariner 10 data set were determined. With these new parameters the following search strategy was adopted: (1) For each pixel in the output coverage map, compute the corresponding  $(\lambda, \phi)$  point and extract a list of the records of images covering this location. (2) Remove records of images from this list where the Sun was below the horizon or where the spacecraft was  $< 15^{\circ}$  in elevation. (3) For

the remaining images, examine all possible stereo pair permutations and eliminate stereo pairs according to these three rules: The image resolution (projected image pixel size on the planet) ratio between images should be  $< 3.0$  (this is increased slightly over a value used in earlier work [Cook *et al.*, 1992] to cater for the smaller quantity of images available). Accept only stereo pairs with a height accuracy of better than  $\pm 1000$  m. The stereo angle should be  $< 1.5$  times the average elevation angle of the two images. (4) Find the smallest stereo accuracy for all the pairs examined for the given  $(\lambda, \phi)$  point and output to the stereo coverage map. (5) Repeat steps 1–5 for other parts of the map.

From the final run, using the parameters listed above, 2326 valid stereo pairs were identified. However, some of these pairs are not useful because they overlap in too small an area, making them impractical for stereo matching. The stereo coverage map derived from this search (Plate 1) illustrates the best stereo height accuracy that can be obtained from Mariner 10

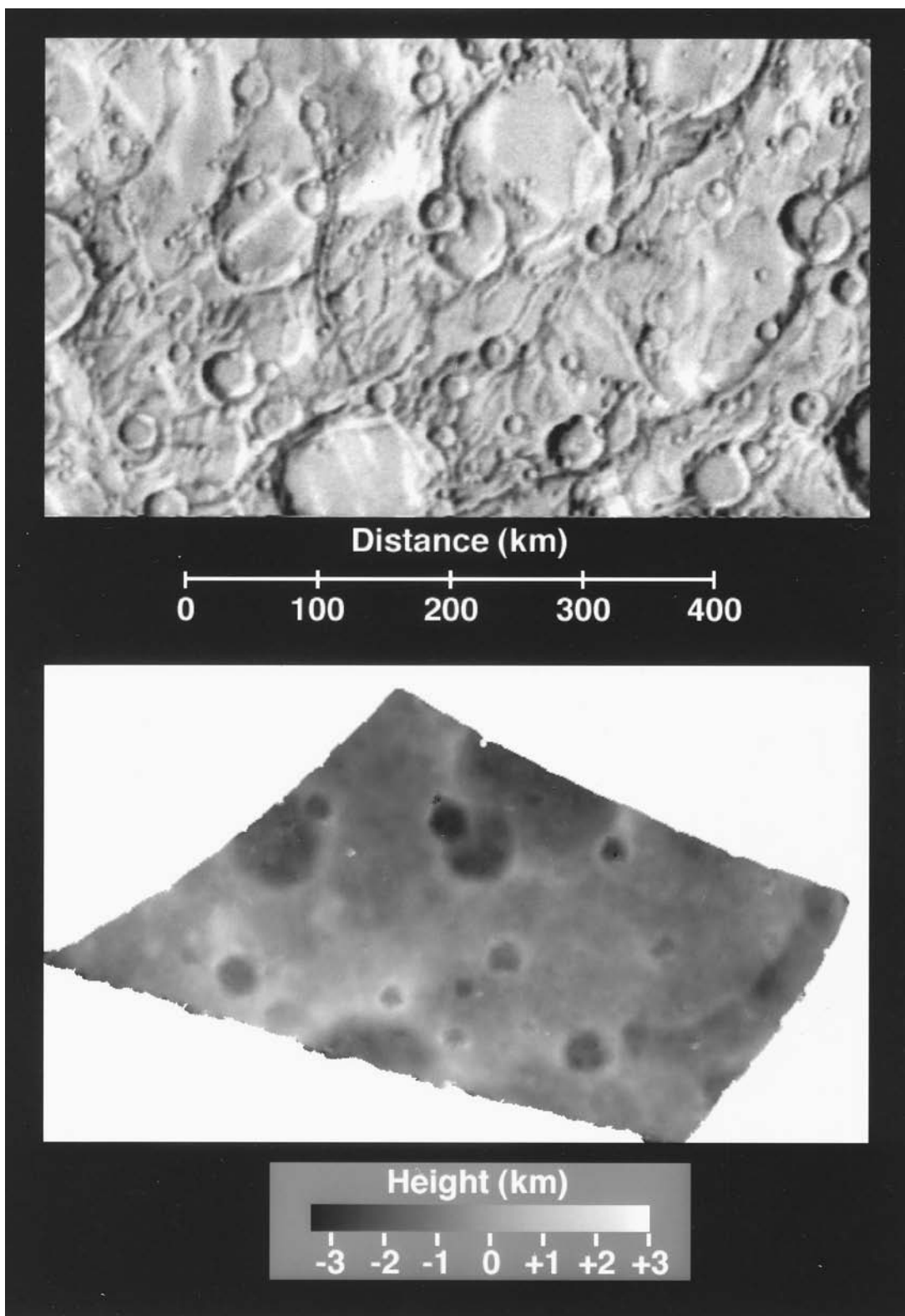


**Figure 10.** Comparison of (top) an airbrush map and (bottom) DEM of the Discovery Rupes area. The Discovery Rupes DEM is one of the highest-quality DEMs that has been produced thus far for Mercury. The two images used were images 027399 and 166613. The region of the gray scale DEM is 62°W–36°W, 60°S–51.5°S (white indicates areas that lie outside the stereo pair overlap or that could not be stereo matched reliably). The predicted stereo height accuracy for this image pair is  $\pm 570$  m.

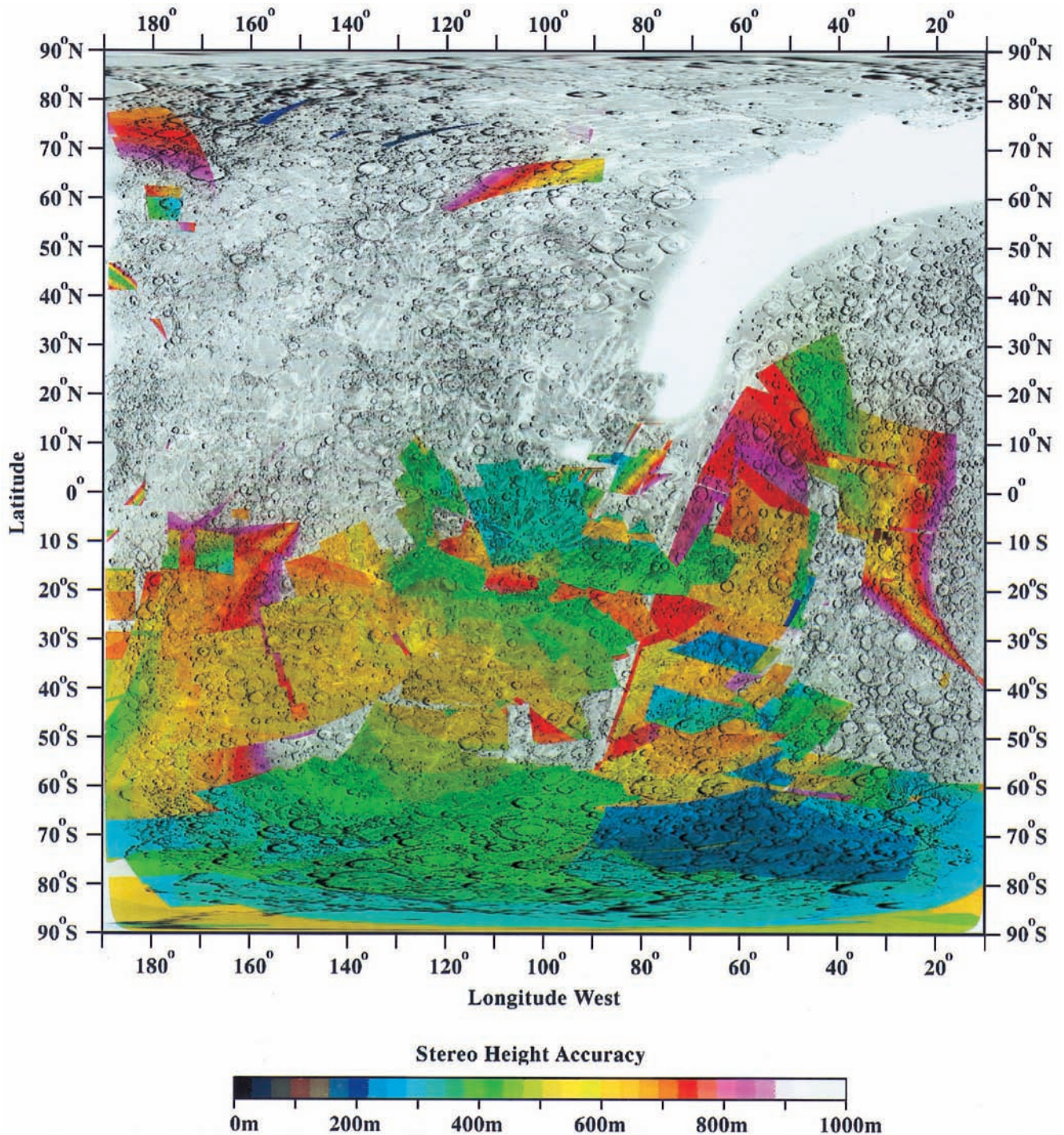


**Plate 1.** Simple cylindrical map projection showing the stereo height accuracy and coverage available for Mercury. Blue and green colors indicate regions where good stereo height accuracy exist. White and pink areas show where poorer stereo height accuracy can be found.

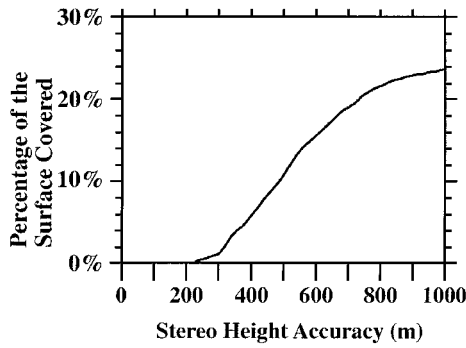


**Figure 11.** Plot of the percentage of the surface of Mercury covered at different stereo height accuracies. No imagery is included where the solar elevation angle was below the horizon or where the spacecraft was  $<15^\circ$  in elevation.

stereo pairs. Areas with good stereo height accuracy (below 350 m) are colored light blue. Areas with poor stereo accuracy are pink, representing 750 m to 1000 m in stereo height accuracy. The northern hemisphere is poorly covered mostly because of the geometry between first and second flybys [Murray et al., 1974; Strom et al., 1975]. The bulk of the northern hemisphere coverage is in the Kuiper H-6 map sheet area, but elsewhere there are some isolated patches at  $70^\circ\text{N}$  and a small patch on the edge of the Caloris basin. Extensive sections of the southern hemisphere are covered, apart from 50% of the H-11 Discovery map sheet and a few isolated patches on other map sheets. Approximately 24% of the planet can be mapped

topographically to better than  $\pm 1$  km height accuracy (for a single matched point: see below), and 6% of the surface can be mapped to better than  $\pm 400$  m height accuracy (Figure 11).

**6. Discussion and Conclusion**

Although Mariner 10, like many earlier space missions, did not carry a special purpose wide-angle cartographic camera as on the Apollo missions [Doyle, 1972; Wu et al., 1972; McEwen and Clanton, 1973; Greeley and Batson, 1990], useful topographic information can be gleaned using stereo analysis [Dzurisin, 1978; Malin, 1978; Thompson et al., 1986; Watters et al., 1998]. The stereo coverage map (Plate 1) shows the best stereo height accuracy from any image pair that can be obtained over the imaged portion of Mercury. Using photogrammetric block adjustment, it is possible to combine the matched points from several overlapping images. The net result is that both the relative and absolute height accuracy of the resulting digital terrain model can be improved. For example, if there were four stereo pairs of similar height accuracy, by combining these, the height accuracy in the DEM would be improved by approximately a factor of 2. By increasing the pixel size in the output DEM, a greater number of height points may be combined, thus improving the DEM signal-to-noise ratio at the expense of spatial resolution. Table 1 lists 20 examples of good-quality Mariner 10 stereo pairs available for Mercury. The DEMs from three of these pairs are shown (Figures 3, 9, and 10).

The stereo coverage map is intended to help identify which areas on Mercury can be automatically stereo matched using

**Table 1.** Twenty Examples of Mariner 10 Stereo Pairs That Yield Good-Quality DEMs

Image 1	Image 2	Min. Height Accuracy, m	Max. Height Accuracy, m	Min. Image Resolution, m	Max. Lon., deg	Min. Lon., deg	Max. Lat., deg	Min. Lat., deg	Min. Elevat. Angle, deg	Stereo Angle, deg	Map Sheet	Nearest Feature
000080	529045	295	460	368	181	176	59	54	46	8	H-3	Brahms
000125	166912	299	430	772	171	164	-13	-16	49	39	H-8	Tolstoj basin
000148	529086	449	982	533	115	73	66	61	15	5	H-3	...
000149	529086	465	998	532	126	93	57	66	15	5	H-3	Botticelli south
000207	166815	431	491	706	127	114	-14	-26	15	61	H-7	Beethoven basin east
027398	166613	510	553	668	45	37	-59	-53	35	41	H-11	Discovery Rupes
027399	166613	518	614	668	63	36	-51	-60	27	41	H-11	Discovery Rupes
166643	027301	559	580	806	69	53	-11	-25	21	46	H-6	Repin
166652	027417	291	336	559	83	68	-39	-47	15	52	H-11	Astrolabe Rupes
166687	166621	531	723	647	71	33	-69	-81	54	21	H-15	Sadi
166744	166835	368	442	556	155	136	-57	-64	41	40	H-12	south of Vincente
166750	166836	339	404	556	163	142	-56	-66	37	38	H-12	Pourquois-Pas Rupes
166752	166689	315	373	484	157	39	-79	-88	39	31	H-15	NE of Chao Meng-Fu
166749	166835	338	400	557	157	133	-61	-72	33	38	H-12	
166776	166639	377	410	598	80	70	-12	-20	41	60	H-7	Rapheal north
166778	166691	346	381	481	86	81	-10	-16	46	43	H-7	north of Futabatei
166779	166876	409	485	666	99	90	-8	-19	34	33	H-7	...
166781	166693	337	350	480	99	92	0	-10	34	44	H-7	...
166912	000241	645	796	832	176	161	-12	-26	40	36	H-8	Tolstoj basin south
166913	000245	685	999	846	174	160	-17	-4	48	36	H-8	Tolstoj basin north

the available Mariner 10 images. For manual stereo viewing purposes, the stereo coverage map helps to eliminate areas that are unsuitable because the stereo angles are too weak or too strong. However, it is possible that a few of the remaining areas may prove also unsuitable because the human visual stereo system cannot cope with the wide range of viewing angles and resolution ratios that can be accommodated by automated matching algorithms [e.g., Day *et al.*, 1992]. A list of stereo pairs and the stereo coverage map are available via the National Air and Space Museum web site at <http://www.nasa.gov/ceps/research/cook/topomerc.html>.

For future missions to Mercury, picture sequences could be planned such that new images can be combined with images from Mariner 10 in order to constitute stereo pairs for the northern hemisphere as seen by Mariner 10. Such planning would be prudent for initial flybys or in case the mission terminates before new global stereo coverage is obtained. Such stereo pairs would be optimal if the difference in elevations and azimuths of the Sun will be less than 15° and 45°, respectively [Cook *et al.*, 1992].

**Acknowledgments.** The authors would like to thank Mert Davies (RAND) for helpful discussions, University College London/Laser-Scan for permission to use the stereo-matching software developed by Tim Day, and Tom Watters (NASM) for helpful comments on the paper.

## References

- Belton, M. J. S., *et al.*, Galileo multispectral imaging of the north pole and eastern limb regions of the Moon, *Science*, 264, 1112–1115, 1994.
- Benesh, M., and M. Morrill, MVM '73 subsystem calibration report, *JPL Doc. 615-148*, Jet Propul. Lab., Pasadena, Calif., 1973.
- Cook, A. C., T. Day, J.-P. Muller, J. C. Iliffe, D. A. Rothery, G. D. Thornhill, and J. B. Murray, A Prolog-based Mars information system, *Int. Arch. Photogramm. Remote Sens.*, 29-B4, 788–794, 1992.
- Cook, A. C., T. Roatsch, J. Oberst, and H. Hoffmann, Semi-automated extraction of DTMs for studies of the lunar surface using Apollo Metric and Clementine stereo pair imagery (abstract), *Bull. Am. Astron. Soc.*, 26, 1097, 1994a.
- Cook, A. C., E. Hauber, R. Pischel, K. Eichertop, and G. Neukum, A versatile geographic information system for use in planetary science, *Int. Arch. Photogramm. Remote Sens.*, 30-4, 556–563, 1994b.
- Cook, A. C., J. Oberst, T. Roatsch, R. Jaumann, and C. Acton, Clementine imagery: Selenographic coverage for cartographic and scientific use, *Planet. Space Sci.*, 44, 1135–1148, 1996.
- Cook, A. C., M. S. Robinson, and J. Oberst, Assessment of Mariner 10 stereo images of Mercury (abstract), *Proc. Lunar Planet. Sci. Conf.*, 28th, 253–254, 1997.
- Cook, A. C., T. R. Watters, M. S. Robinson, P. D. Spudis, and D. B. J. Bussey, Lunar polar topography derived from Clementine stereo images, *J. Geophys. Res.*, in press, 2000.
- Danielson, G. E., K. P. Klaasen, and J. L. Anderson, Acquisition and description of Mariner 10 television science data at Mercury, *J. Geophys. Res.*, 80, 2357–2393, 1975.
- Davies, M. E., S. E. Dwornik, D. E. Gault, and R. G. Strom, *Atlas of Mercury*, NASA Spec. Publ., SP-423, 127 pp., 1978.
- Davies, M. E., T. R. Colvin, M. S. Robinson, and K. Edwards, Mercury's polar regions: Locations of radar anomalies (abstract), *Bull. Am. Astron. Soc.*, 28, 1115, 1996.
- Davis, P. A., and L. A. Soderblom, Modeling crater topography and albedo from monoscopic Viking Orbiter images, *J. Geophys. Res.*, 89, 9449–9457, 1984.
- Day, T., A. C. Cook, and J.-P. Muller, Automated digital topographic mapping techniques for Mars, *Int. Arch. Photogramm. Remote Sens.*, 29-B4, 801–808, 1992.
- Doyle, F. J., Photogrammetric analysis of Apollo 15 records, in *Apollo 15 Preliminary Science Report*, NASA Spec. Publ., SP-289, 25–27–25–48, 1972.
- Dunne, J. A., and E. Burgess, *The Voyage of Mariner 10*, NASA Spec. Publ., SP-424, 221 pp., 1978.
- Dzurisin, D., The tectonic and volcanic history of Mercury as inferred from studies of scarps, ridges and troughs and other lineaments, *J. Geophys. Res.*, 83, 4883–4906, 1978.
- Eliason, E., and A. S. McEwen, Adaptive box filters for removal of random noise from digital images, *Photogramm. Eng. Remote Sens.*, 56, 453–456, 1990.
- Giese, B., J. Oberst, R. L. Kirk, and W. Zeitler, High resolution digital terrain models of asteroid Ida: A comparison between photogrammetry and the shape from shading method (abstract), *Proc. Lunar Planet. Sci. Conf.*, 27th, 409–410, 1996.
- Greeley, R., and R. M. Batson (Eds.), *Planetary Mapping*, Cambridge Planet. Sci. Ser., vol. 6, 296 pp., Cambridge Univ. Press, New York, 1990.
- Hapke, B., E. Danielson, K. Klaasen, and L. Wilson, Photometric observations of Mercury from Mariner 10, *J. Geophys. Res.*, 80, 2431–2443, 1975.
- Harmon, J. K., D. B. Campbell, D. L. Bindschadler, J. W. Head, and I. I. Shapiro, Radar altimetry of Mercury: A preliminary analysis, *J. Geophys. Res.*, 91, 385–401, 1986.
- Jet Propulsion Laboratory (JPL), MVM '73 stereo data package user guide, Pasadena, Calif., Jan. 5, 1976.
- Kirk, R. L., I, Thermal evolution of Ganymede and implications for surface features, II, Magnetohydrodynamic constraints on deep zonal flow in the giant planets, III, A fast finite-element algorithm for two-dimensional photoclinometry, Ph. D. thesis, 274 pp., Calif. Inst. of Technol., Pasadena, 1987.
- Malin, M. C., Surfaces of Mercury and the Moon: Effects of resolution and lighting conditions on the discrimination of volcanic features, *Proc. Lunar Planet. Sci. Conf.*, 9th, 3395–3409, 1978.
- Malin, M. C., and D. Dzurisin, Landform degradation on Mercury, the Moon, and Mars: Evidence from crater depth/diameter relationships, *J. Geophys. Res.*, 82, 376–388, 1977.
- McEwen, A. S., Photometric functions for photoclinometry and other applications, *Icarus*, 92, 298–311, 1991.
- McEwen, A. S., and M. S. Robinson, Mapping of the Moon by Clementine, *Adv. Space Res.*, 19(10), 1523–1533, 1997.
- McEwen, M. C., and U. S. Clanton, Photographic summary, in *Apollo 17 Preliminary Science Report*, NASA Spec. Publ., SP-330, 4-1–4-32, 1973.
- Mouginis-Mark, P. J., and L. Wilson, MERC: A FORTRAN IV program for the production of topographic data for the planet Mercury, *Comput. Geosci.*, 7, 35–45, 1981.
- Murray, B. C., The Mariner 10 pictures of Mercury: An overview, *J. Geophys. Res.*, 80, 2342–2344, 1975.
- Murray, B., and E. Burgess, *Flight to Mercury*, 162 pp., Columbia Univ. Press, New York, 1977.
- Murray, B. C., M. J. S. Belton, G. E. Danielson, J. E. Davies, D. E. Gault, B. Hapke, B. O'Leary, R. G. Strom, V. Suomi, and N. Trask, Mercury's surface: Preliminary description and interpretation from Mariner 10 pictures, *Science*, 185, 169–179, 1974.
- Murray, J. B., D. A. Rothery, G. Thornhill, J.-P. Muller, T. Cook, T. Day, and J. C. Iliffe, The origin of grooves and crater chains of Phobos (abstract), *Proc. Lunar Planet. Sci. Conf.*, 23rd, 949–950, 1992.
- Oberst, J., T. Roatsch, W. Zhang, A. C. Cook, R. Jaumann, T. Duxbury, F. Wewel, R. Uebbing, F. Scholten, and J. Alibert, Photogrammetric analysis of Clementine multi-look-angle images obtained near Mare Orientale, *Planet. Space Sci.*, 44, 1123–1133, 1996.
- Pike, R. J., Geomorphology of impact craters on Mercury, in *Mercury*, edited by F. Vilas, C. R. Chapman, and M. S. Matthews, pp. 165–273, Univ. of Ariz. Press, Tucson, 1988.
- Robinson, M. S., B. R. Hawke, P. G. Lucey, and G. A. Smith, Mariner 10 multispectral images of the eastern limb and farside of the Moon, *J. Geophys. Res.*, 97, 18,265–18,274, 1992.
- Robinson, M. S., M. E. Davies, T. R. Colvin, and K. E. Edwards, A new controlled albedo map of Mercury (abstract), *Proc. Lunar Planet. Sci. Conf.*, 28th, 1187–1188, 1997.
- Robinson, M. S., M. E. Davies, T. R. Colvin, and K. Edwards, A revised control network for Mercury, *J. Geophys. Res.*, 104, 30,847–30,852, 1999a.
- Robinson, M. S., A. S. McEwen, E. Eliason, E. M. Lee, E. Malaret, and P. G. Lucey, Clementine UVVIS global mosaic: A new tool for understanding the lunar crust, *Proc. Lunar Planet. Sci. Conf.* [CD-ROM], 30th, abstract 1931, 1999b.

- Schenk, P., and H. J. Melosh, Lobate thrust scarps and the thickness of Mercury's lithosphere (abstract), *Proc. Lunar Planet. Sci. Conf.*, 25th, 1203–1204, 1994.
- Soha, J. M., D. J. Lynn, J. L. Lorre, J. A. Mosher, N. N. Thayer, D. E. Elliott, W. D. Benton, and R. E. Dewar, IPL processing of the Mariner 10 images of Mercury, *J. Geophys. Res.*, 80, 2394–2414, 1975.
- Strom, R. G., et al., Preliminary imaging results from the second Mercury encounter, *J. Geophys. Res.*, 80, 2345–2356, 1975.
- Thompson, D., P. E. Clarke, and M. Leake, Characterization of linear structures on Mercury, paper presented at Mercury Conference, Div. for Planet. Sci., Am. Astron. Soc., Tucson, Ariz., August 1986.
- Watters, T. R., M. S. Robinson, and A. C. Cook, Topography of lobate scarps on Mercury: New constraints on the planet's contraction, *Geology*, 26, 991–994, 1998.
- Wu, S. C. C., Mars synthetic topographic mapping, *Icarus*, 33, 417–440, 1978.
- Wu, S. S. C., F. J. Schafer, R. Jordan, and G. M. Nakata, Photogrammetry using Apollo 16 orbital photography, in *Apollo 16 Preliminary Science Report, NASA Spec. Publ.*, SP-315, 30-5–30-10, 1972.
- 
- A. C. Cook, Center for Earth and Planetary Studies, National Air and Space Museum, Smithsonian Institution, Washington, D. C. 20560-0315. (tcook@ceps.nasm.edu)
- M. S. Robinson, Department of Geological Sciences, Northwestern University, Locy Hall 309, 1847 Sheridan Road, Evanston, IL 60208. (robinson@earth.nwu.edu)

(Received June 29, 1999; revised December 3, 1999; accepted December 21, 1999.)

